Research Paper
Computational Methods for Differential Equations
http://cmde.tabrizu.ac.ir
Vol. *, No. *, *, pp. 1-10
DOI:10.22034/cmde.2025.67639.3231

Forecasting disease spread using the stochastic model and Kalman filter

Javad Hajizadeh and Parisa Nabati*
Faculty of Science, Urmia University of Technology, Urmia, Iran.

Abstract

This manuscript investigates the use of stochastic differential equations alongside Kalman filtering methodologies within the SIRD framework to enhance the predictive accuracy of infectious disease epidemic modeling. Leveraging empirical data from the COVID-19 pandemic, the study incorporates stochasticity into transmission dynamics by introducing perturbations in the infection rate. A comparative analysis of both deterministic and stochastic versions of the model is presented. The extended Kalman filter is employed to infer system states from noisy observations, enabling real-time epidemic monitoring. Simulation results show that applying the Kalman filter significantly improves predictive accuracy and model fidelity, closely aligning with the simulated data. This integrated modeling approach offers a robust framework for public health planning, providing more reliable forecasts and supporting the timely implementation of intervention measures.

Keywords. Stochastic Differential Equations, Kalman Filter, Epidemic Modeling, Prediction, Infectious Diseases.
2010 Mathematics Subject Classification. 60H10, 92B05, 37H10.

1. Introduction

The spread of epidemic diseases causes the death of millions and imposes significant healthcare costs. The success in eradicating such emerging diseases depends not only on medical infrastructure but also on the understanding of the transmission dynamics of a specific disease and the effective implementation of control strategies. Additionally, logistical experiments can influence how the disease is managed. Mathematical models, while unable to fully compensate for real-world losses, offer a powerful tool for testing various scenarios without the associated human or financial cost.

Over the past few decades, researchers have proposed models based on differential equations to describe biological phenomena, including disease transmission. These models help understand the characteristics of infectious disease transmission, predict their trends, and assess their impact on human health. Given the destructive and threatening nature of epidemic diseases, employing mathematical models for studying epidemics is essential. Mathematical models, particularly compartmental models like SIR and its variants, have long been employed to understand transmission dynamics and evaluate the impact of intervention strategies [1, 5]. These models help policymakers simulate various scenarios and formulate data-driven strategies without incurring real-world human or economic losses [4, 9].

Among the compartmental models, the SIRD model (Susceptible-Infected-Recovered-Deceased) is particularly well-suited for diseases with significant mortality, such as COVID-19 [13]. While deterministic models provide a foundational framework, they often fail to capture the inherent randomness in real-world epidemiological processes, such as fluctuations in contact rates or variability in disease reporting.

To incorporate such uncertainties, researchers have turned to stochastic differential equations (SDEs) that allow the inclusion of noise and randomness in model parameters. For instance, stochastic versions of the SIRD and SEIR models have been enhanced using processes like the Ornstein–Uhlenbeck mean-reverting process, which better reflects environmental and behavioral fluctuations [7, 10, 17]. These models are particularly valuable in early outbreak stages when data are sparse and highly variable [18].

Received: 01 June 2025; Accepted: 14 April 2026.
∗ Corresponding author. Email: p.nabati@uut.ac.ir.

Stochastic models in disease forecasting such as the SIRD-V, SIQR and SEIHCRDV, incorporate randomness to reflect the unpredictable nature of disease spread, capturing variations in transmission and recovery rates [12, 14, 19, 20]. These models utilize probability generating functions to analyze the impact of interventions over time, allowing for a nuanced understanding of epidemic dynamics.

Moreover, the integration of filtering techniques such as the Kalman filter has further enhanced the applicability of epidemic models by enabling real-time estimation of unobservable variables (e.g., actual infections) and improving the predictive performance of models through noise reduction [3, 21]. The extended Kalman filter (EKF) and its variants, like the Unscented Kalman Filter (UKF), allow for dynamic adjustment of model parameters in response to new data, making them particularly effective during fast-evolving pandemics [15].

Stochastic models and the Kalman filter play crucial roles in enhancing the understanding and prediction of epidemic dynamics. Stochastic models account for the inherent randomness in disease transmission, particularly during the early stages of an outbreak when the number of infectious individuals is low. The Kalman filter, a recursive estimation technique, is employed to update model parameters in real-time as new data becomes available, improving the accuracy of predictions and parameter estimates [6].

Kalman-based approaches have already proven effective in modeling a range of diseases, including COVID-19 and HIV, by reducing uncertainty in predictions and enhancing the understanding of disease trajectories under different control strategies [2, 3]. These hybrid stochastic-Kalman models not only improve forecast accuracy but also help health authorities anticipate critical thresholds in the progression of an epidemic, such as the peak number of infections or the saturation of healthcare capacity. The Kalman filter is utilized to incorporate real-time data into epidemic models, allowing for dynamic adjustments to parameters based on observed fluctuations in disease incidence [16]. It has been shown to improve parameter estimation significantly, especially in the presence of measurement errors and incomplete data, outperforming traditional methods like least squares [8].

While stochastic models and the Kalman filter offer powerful tools for epidemic modeling, challenges remain, particularly in data availability and the complexity of real-world disease dynamics. Addressing these issues is essential for improving the reliability of epidemic forecasts and public health responses.

In this study, we develop a stochastic extension of the SIRD model by introducing random perturbations into the infection rate, modeled using a white noise process. The model is further augmented using the EKF, which enables real-time estimation of model states from noisy observations. Our goal is to demonstrate that this hybrid approach significantly enhances the accuracy and reliability of epidemic forecasts. The structure of the paper is as follows: Section 2 introduces the deterministic and stochastic formulations of the SIRD model. Section 3 explains how the EKF is used. The analysis and results of the simulation are shown in section 4. The consequences and future work are discussed in section 5's conclusion.

2. Methodology

2.1. **Deterministic SIRD Model.** We consider a compartmental model dividing the population into Susceptible (S), Infected (I), Recovered (R), and Deceased (D). The deterministic form is governed by a system of ordinary differential equations [11].

$$\begin{cases} \frac{dS}{dt} = -\beta(t)S(t)I(t), \\ \frac{dI}{dt} = \beta(t)S(t)I(t) - (\alpha(t)+\gamma(t))I(t), \\ \frac{dR}{dt} = \alpha(t)I(t), \\ \frac{dD}{dt} = \gamma(t)I(t), \end{cases} \tag{2.1}$$

for the start time t_0, with $[S(t_0), I(t_0), R(t_0), D(t_0)]$ serving as the initial condition. The infection rate is denoted by β. The recovery and death rates are denoted by the parameters α and γ, respectively. Now we examine the ordinary

differential equations of the daily discrete nonlinear $SIRD$ model at time k to $k+1$ and we have:

$$\begin{cases} S(k+1) = S(k) - \beta(k)S(k)I(k), \\ I(k+1) = S(k) + \beta(k)S(k)I(k) - \alpha(k)I(K) - \gamma(k)I(k), \\ R(k+1) = R(k) + \alpha(k)I(k), \\ D(k+1) = D(k) + \gamma(k)I(k). \end{cases} \tag{2.2}$$

In the above equations, $\alpha(k)$, (k), β and $\gamma(k)$ are the daily recovery rate, daily infection rate and daily death rate, respectively. These daily rates are optimized using the least squares method (LSM) as follows:

$$\begin{cases} \alpha(k) = \frac{\sum_{j=1}^{k} I(j)\Delta R(j)}{\sum_{j=1}^{k} I(j)}, \\ \beta(k) = \frac{\sum_{j=1}^{k} I(j)\Delta S(j)}{\sum_{j=1}^{k} I(j)}, \\ \gamma(k) = \frac{\sum_{j=1}^{k} I(j)\Delta D(j)}{\sum_{j=1}^{k} I(j)}, \end{cases} \tag{2.3}$$

and in these equations we have:
$I(j)$ is the total number of current infections at time j.
$\Delta S(j) = S(j) - S(j-1)$ represents the number of new infections at time j.
$\Delta R(j) = R(j) - R(j-1)$ represents the number of recoveries at time j.
$\Delta D(j) = D(j) - D(j-1)$ represents the number of deaths due to the disease at time j. We assume:

$$x_1(k) = S(k),\ x_2(k) = I(k),\ x_3(k) = R(k),\ x_4(k) = D(k).$$

Now, based on these assumptions, the SIRD model will be as follows:

$$\begin{cases} x_1(k+1) = f_1(x_k) = x_1(k) - \beta(k)x_1(k)x_2(k), \\ x_2(k+1) = f_2(x_k) = x_2(k) + \beta(k)x_1(k)x_2(k) - \alpha(k)x_2(k) - \gamma(k)x_2(k), \\ x_3(k+1) = f_3(x_k) = x_3(k) + \alpha(k)x_2(k), \\ x_4(k+1) = f_4(x_k) = x_4(k) + \gamma(k)x_2(k). \end{cases} \tag{2.4}$$

2.2. **Stochastic Extension.** To account for uncertainties, we introduce noise into the transmission rate (β), converting the model to a SDE system. Introducing a stochastic component into this model with ODEs is a good idea, since it is assumed that the parameters fluctuate randomly around their mean due to occasional disturbances. A white noise process can be modeled as a Wiener process.

Suppose the infection rate β is not precisely known and is subject to random environmental influences. In that case, we assume: $\beta = \beta + noise$. Thus, if a stochastic component is introduced into the parameters, by substituting the relation $\beta \to \beta + \sigma\xi(t)$, into the model equations, we obtain a system of SDEs of the Ito type for the SIRD model as follows:

$$\begin{cases} \frac{dS}{dt} = -\big(\beta + \sigma\xi(t)\big)S(t).I(t), \\ \frac{dI}{dt} = \big(\beta + \sigma\xi(t)\big)S(t).I(t) - (\alpha + \gamma)I(t), \\ \frac{dR}{dt} = \alpha I(t), \\ \frac{dD}{dt} = \gamma I(t). \end{cases} \tag{2.5}$$

In the above equations, $\xi(t)$ is a white noise process with zero mean and unit variance, and σ is a non-negative constant that is considered as the noise intensity. By considering $\xi(t)dt = dw(t)$ we have:

$$\begin{cases} dS(t) = -\beta S(t)I(t)dt - \sigma s(t)I(t)dw(t), \\ dI(t) = \beta S(t)I(t)dt + \sigma s(t)I(t)dw(t) - \alpha I(t)dt - \gamma I(t)dt, \\ dR(t) = \alpha I(t)dt, \\ dD(t) = \gamma I(t)dt. \end{cases} \tag{2.6}$$

To determine whether the solution is beneficial and universal, we must first look at the dynamic behavior of an epidemic model. The following theorem, which ensures that the solution stays in Δ, will be used in this section to show that the model is well expressed and, therefore, biologically significant.

Theorem 2.1. *There exists a singular solution to system (2.6) for all $t > 0$ almost surely (a.s.). with any initial value.*

Proof. Suppose $X(t) = \big(S(t), I(t), R(t), D(t)\big)$. For every initial value, the coefficients of the system (2.6) are locally lipschitz continuous. As a result, there is only one solution $X(t) \in \Lambda$ on $t \in [0, \tau_e]$, where τ_e is the explosion time.

At this point, we demonstrate that $\tau_e = \infty$ (a.s.) and that the solution is global. Assume that $w_0 > 0$ is sufficiently big to let that every member of $X(0)$ falls inside the interval $[\frac{1}{w_0}, w_0]$. Define,

$$\varrho_{min}(t) = \min\{S(t), I(t), R(t), D(t)\},$$
$$\varrho_{max}(t) = \max\{S(t), I(t), R(t), D(t)\},$$

for any $w \geq w_0$ and

$$\tau_w = \inf\{t \in [0, \tau_e) : \varrho_{min}(t) \leq \frac{1}{w} \text{ or } \varrho_{max}(t) \geq w\},$$

Suppose $\inf \phi = \infty$ which ϕ proposed the empty set. Then τ_w is increasing when $w \to \infty$. We determine that $\tau_\infty \leq \tau_e$ a.s. by setting $\tau_\infty = \lim_{w\to\infty} \tau_w$,. It is evident that if $\tau_\infty = \infty$ a.s., then $X(t) \in \Lambda$ for all $t > 0$, then $\tau_e = \infty$ a.s.

If $\tau_\infty \neq \infty$, then, there exists two constants $\hat{\delta} > 0$ and $\tilde{\upsilon} \in (0, 1)$ such that $P(\tau_\infty \leq \hat{\delta}) \geq \tilde{\upsilon}$. Next,

$$\exists t_1 \in \mathbb{Z}, t_1 > t_0, \quad s.t. \quad P(\tau_e \leq \hat{\delta}) \geq \tilde{\upsilon} \ \ \forall\, t \geq t_1. \tag{2.7}$$

□

Take the function φ, With the definition below, $\varphi : \mathbb{R}^4_+ \to \mathbb{R}_+$ is twice differentiable.

$$\varphi(X(t)) = (S - 1 - \log S) + (I - 1 - \log I) + (R - 1 - \log R) + (D - 1 - \log D).$$

The function φ is non-negative. Using the Ito formula and the system (2.6),

$$d\varphi(X(t)) = \mathcal{L}\varphi(X(t))dt - \sigma I(t)dw(t) - \sigma S(t)dw(t),$$

which

$$\begin{aligned}\mathcal{L}\varphi(X(t)) &= (1 - \frac{1}{S(t)})(-\beta S(t)I(t)) \\ &+ (1 - \frac{1}{I(t)})(\beta S(t)I(t)) \\ &- (1 - \frac{1}{I(t)})(\alpha + \gamma)I(t) + (1 - \frac{1}{R(t)})\alpha I(t) \\ &+ (1 - \frac{1}{D(t)})\gamma I(t) + \sigma^2 I^2(t) + \sigma^2 S^2(t) := \mathcal{Y},\end{aligned}$$

where $\mathcal{Y} \in \mathbb{R}_+$, then

$$\int_0^{\tau_e \wedge \hat{\delta}} d\varphi(X(t)) \leq \int_0^{\tau_e \wedge \hat{\delta}} \mathcal{Y}dt + \int_0^{\tau_e \wedge \hat{\delta}} \sigma I(t)dw(t) + \int_0^{\tau_e \wedge \hat{\delta}} \sigma S(t)dw(t),$$

and

$$\begin{aligned}\mathbb{E}\big(\varphi(X(t))\big) &\leq \mathbb{E}\big(\varphi(X(0))\big) + \mathcal{Y}\mathbb{E}(.) \\ &\leq \mathbb{E}\big(\varphi(X(0))\big) + \mathcal{Y}\hat{\delta},\end{aligned} \tag{2.8}$$

$\mathbb{E}$ is the representation of the mathematical expectation. For $\upsilon \geq \upsilon_1$, let $\Omega_\upsilon := \tau_e \leq \hat{\delta}$. We obtain $P(\Omega_\upsilon) \geq \tilde{\upsilon}$ from Equation(2.7). Define

$$\Lambda_{\tau_e} := \varphi\big(X(\tau_e)\big),$$

then

$$\Lambda_{\tau_e} \geq (w - 1 - \log w) \wedge (\frac{1}{w} - 1 + \log w).$$

Equations (2.7) and (2.8) concluded that:

$$\begin{aligned}\mathbb{E}(\Lambda_0) + \mathcal{Y}\hat{\delta} &\geq \mathbb{E}\big(I_{\Omega_\upsilon}\Lambda_{t_w}\big) \\ &\geq \tilde{\upsilon}[(w - 1 - \log w) \wedge (\frac{1}{w} - 1 + \log w)].\end{aligned}$$

Where the indicator of the set Ω_τ is I_{Ω_τ}. If $\upsilon \to \infty$ we have $\infty > \mathbb{E}(\Lambda_0) + \mathcal{Y}_{\hat{\delta}} = \infty$, this is a contradiction. In such case, $\tau_\infty = \infty$ a.s. and the hypothesis $P(\tau_\infty \leq \hat{\delta} > \tilde{w}$ is false.

The system (2.6) is nonlinear. However, the Kalman filter operates with linear system equations. Therefore, to transform the SDE into a linear form, we use the EKF.

2.3. **Extended Kalman Filter.** The Extended Kalman Filter (EKF) is a widely used nonlinear extension of the classical Kalman Filter, designed to handle systems with nonlinear dynamics and observation models. While the traditional Kalman Filter is suitable for linear systems, the EKF adapts it to nonlinear systems by performing local linearization using first-order Taylor series expansion.

In the context of epidemic modeling, the EKF approximates the nonlinear state transition and observation functions by evaluating their Jacobians at the current state estimates. The general form of the EKF model is expressed as:

$$\begin{aligned}\mathbf{x}_k &= f(\mathbf{x}_{k-1}, \mathbf{u}_{k-1}) + \mathbf{w}_{k-1}, \\ \mathbf{z}_k &= h(\mathbf{x}_k) + \mathbf{v}_k,\end{aligned}$$

where

- $\mathbf{x}_k$: state vector,
- $\mathbf{u}_k$: control input,
- $\mathbf{z}_k$: measurement vector,
- $\mathbf{w}_k \sim \mathcal{N}(0, Q_k)$: process noise,
- $\mathbf{v}_k \sim \mathcal{N}(0, R_k)$: measurement noise.

The EKF operates in two primary stages: prediction and update.

Prediction Step:

$$\hat{x}_{k|k-1} = f(\hat{x}_{k-1|k-1}, u_{k-1}) \tag{2.9}$$

$$F_{k-1} = \left.\frac{\partial f}{\partial x}\right|_{\hat{x}_{k-1}, u_{k-1}} \tag{2.10}$$

Update Step:

$$H_k = \left.\frac{\partial h}{\partial x}\right|_{\hat{x}_{k|k-1}}, \tag{2.11}$$

$$y_k = z_k - h(\hat{x}_{k|k-1}), \tag{2.12}$$

$$S_k = H_k P_{k|k-1} H_k^\top + R_k, \tag{2.13}$$

$$K_k = P_{k|k-1} H_k^\top S_k^{-1}, \tag{2.14}$$

$$\hat{x}_{k|k} = \hat{x}_{k|k-1} + K_k y_k, \tag{2.15}$$

$$P_{k|k} = (I - K_k H_k) P_{k|k-1}. \tag{2.16}$$

At each time step, the Jacobian matrices F_k and H_k are computed using the predicted states. These matrices are crucial for linearizing the nonlinear system dynamics and measurements around the current estimate.

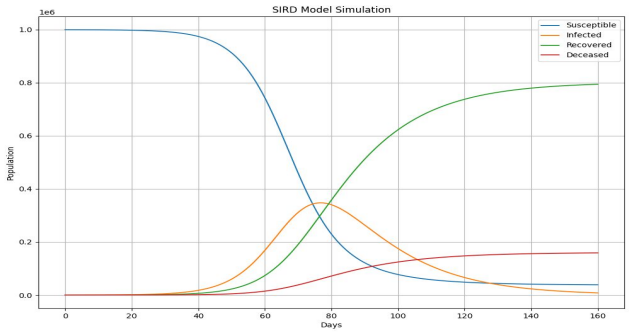

FIGURE 1. The deterministic Sird model.

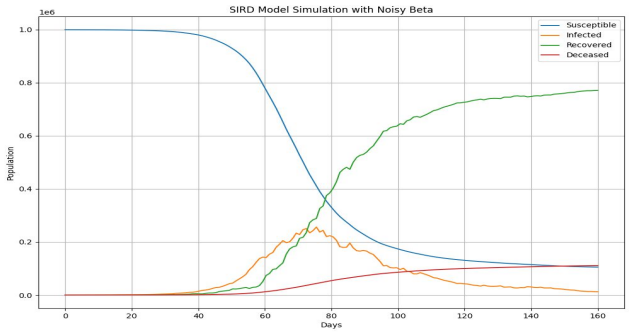

FIGURE 2. The stochastic SIRD model with noisy β.

For the stochastic SIRD model expressed in Equation (2.6), the Jacobian matrix F used in the EKF is derived as follows:

$$F = \begin{bmatrix} 1-\beta I(k) & -\beta S(k) & 0 & 0 \\ \beta I(k) & 1+\beta S(k)I(k)-(\alpha+\gamma) & 0 & 0 \\ 0 & \alpha & 1 & 0 \\ 0 & \gamma & 0 & 1 \end{bmatrix}. \tag{2.17}$$

This matrix facilitates the local linearization of the nonlinear stochastic system, enabling effective state estimation through the EKF framework.

3. Numerical Simulation

In this section, the results obtained from the simulation are examined and analyzed. At first, we review the SIRD model and its graphs based on simulated data. Then, the graphs resulting from the SDE with noise are analyzed. Subsequently, the cumulative simulated graphs of the model, processed using the EKF, are evaluated and the results are examined. Finally, all three types of graphs, those based on simulated data, the noisy graphs, and the simulated graphs using the Kalman filter are compared and analyzed together, and the conclusions drawn from the charts are presented.

Consider a SIRD model with $S(0) = 0.75,\ I(0) = 0.25,\ R(0) = 0,\ D(0) = 0$ and $\alpha = 0.15, \beta = 0.1,\ \gamma = 0.1,\ \xi = 0.25,\ \theta = 0.4,\ \bar{\alpha} = 0.22,\ \sigma = 0.1$. The camulative graph is shown in Figure 1. Figure 2 shows the stochastic model with noisy parameter. Figure 3 presents the model's predictive charts generated by the EKF. The predicted outcomes

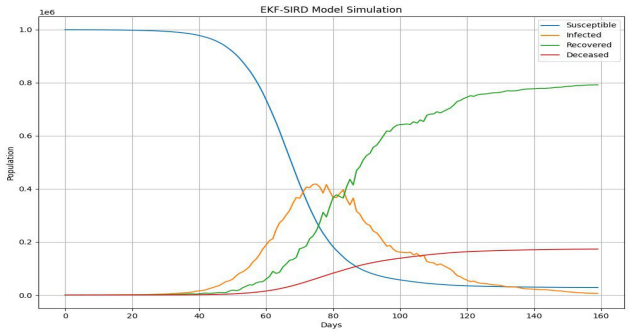

FIGURE 3. The simulated stochastic model using the EKF.

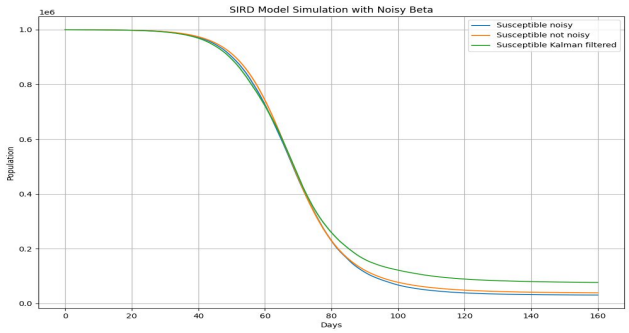

FIGURE 4. The rate of susceptible people.

closely match the actual data, underscoring the value of simulation in disease modeling. Simulation allows for early estimation of the trajectories of the S, I, R, and D compartments at the onset of an epidemic, enabling informed decision-making to protect public health and optimize the use of available resources for disease prevention. The overall structure of the real data trends remains largely preserved in the simulation results. Minor discrepancies between the simulated and actual data charts are attributable to the inherent estimation errors of the EKF.

In the analyses based on real data, the equations with noise term β and the simulation using the EKF, all the plots in Figure 4 related to the susceptible individuals $S(t)$ exhibit a downward trend. The only differences between the real data chart and the simulated or noisy charts stem from the level of error and unknown random effects. As can be seen, in this case as well, the prediction chart produced by the EKF closely aligns with both the noisy data and the real observations, demonstrating the effectiveness and significance of the extended Kalman filter.

The plot in Figure 5 corresponding to the infected individuals $I(t)$ all exhibit both an ascending and a descending phase. The number of infected individuals reaches its peak in the Kalman filter prediction chart, while it is at its lowest in the noisy data chart. The prediction generated by the EKF implies that more intensive preventive measures are required to effectively control the disease.

The plot in Figure 6 related to the recovered individuals $R(t)$ show an upward trend. The only differences between the real data chart and the simulated or noisy charts are due to the level of error and unknown random effects.

The plot in Figure 7 related to deceased individuals $D(t)$ show an upward trend. The EKF predicts the highest number of deaths in this group. According to the figure, the white noise introduced into the disease model has had no significant effect on the increase in mortality rates.

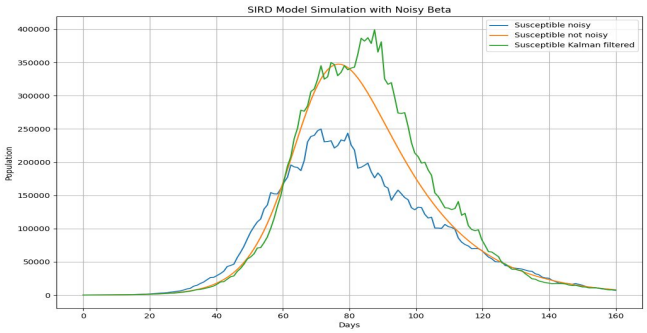

FIGURE 5. The rate of infected people.

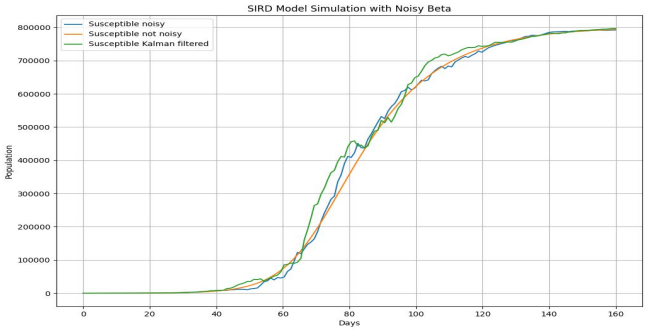

FIGURE 6. The rate of recovered people.

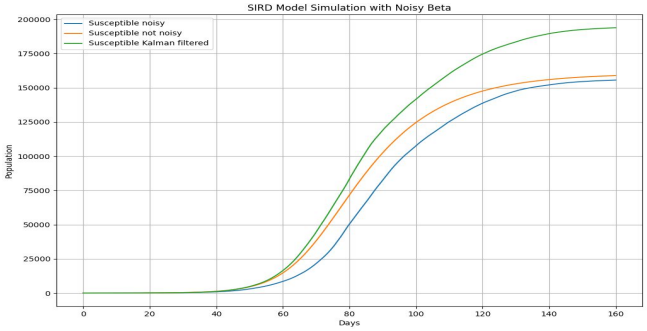

FIGURE 7. The rate of death people.

4. CONCLUSIONS

This study presented an integrated approach combining the classical SIRD epidemiological model with the Kalman filter to enhance the accuracy of infectious disease modeling and prediction. By leveraging the strength of the Kalman filter in dealing with noisy, real-time data, we successfully demonstrated its ability to dynamically estimate the key

compartments of the SIRD model with improved stability and responsiveness compared to traditional numerical methods.

Through simulations and numerical analysis, we observed that the Kalman filter could adapt to changes in disease dynamics over time, making it a powerful tool for short-term forecasting and real-time monitoring during outbreaks. The model effectively reduced the estimation error, thereby providing more reliable predictions for public health decision-making.

While our findings underscore the utility of this hybrid approach, there remain opportunities for further research. Future work could extend this framework to more complex compartmental models such as SEIR or incorporate time-varying transmission rates and external interventions. Additionally, applying this model to real epidemiological data would help validate its robustness in practical settings.

In conclusion, the combining of Kalman filter with the SIRD model offers a promising pathway for enhancing epidemic forecasting capabilities, contributing to better-informed responses in the face of emerging infectious diseases.

References

[1] N. T. J. Bailey, *The Mathematical Theory of Infectious Diseases and Its Applications*, New York: Hafner Press, (1975).

[2] Y. Cai, J. Jiao, Z. Gui, Y. Liu, and W. Wang, *Environmental variability in a stochastic epidemic model*, Applied Mathematics and Computation, *329* (2018), 210–226.

[3] P. Giamberardino and D. Iacoviello, *Early estimation of the number of hidden HIV infected subjects: An extended Kalman filter approach*, Infectious Disease Modelling, *8* (2023), 341–355.

[4] T. Kar and A. Batabyal, *Stability analysis and optimal control of an SIR epidemic model with vaccination*, Biosystems, *104*, 127–135.

[5] W. O. Kermack and A. G. McKendrick, *A contribution to the mathematical theory of epidemics*, Proceedings of the Royal Society of London, Series A, *115*(772), 700–721.

[6] S. Kumar Nanda, G. Kumar, V. Bhatia, and A. Kumar Singh, *Kalman-based compartmental estimation for covid-19 pandemic using advanced epidemic model*, Biomedical Signal Processing and Control, *84* (2023), 104727.

[7] A. Laaribi, B. Boukanjime, M. Khalifi, D. Bouggar, and M. El Fatini, *A generalized stochastic SIRS epidemic model incorporating mean-reverting Ornstein–Uhlenbeck process*, Physica A journal, *615* (2023).

[8] T. Li, H. Rahmandad, and J. D. Sterman, *Improving Parameter Estimation of Epidemic Models: Likelihood Functions and Kalman Filtering*, Social Science Research Network, (2022).

[9] T. Malik and O. Sharomi, *Optimal control in epidemiology. Annals of Operations Research*, *251*, (2015), 55–71.

[10] P. Nabati, *Introducing a Novel Mean-Reverting Ornstein-Uhlenbeck Proccess Based Stochastic Epidemic Model*, Scientific Reports, *14* (2024).

[11] P. Nabati and A. Hajrajabi, *Nonlinear stochastic model for epidemic disease prediction by optimal filtering perspective*, Math. Meth. Appl. Sci., (2024), 1-17.

[12] T. Odagaki, *Analysis of the outbreak of COVID-19 in Japan by SIQR model*, Infectious Disease Modelling, *5* (2021), 691-698.

[13] V. Papageorgiou and G. Tsaklidis, *An improved epidemiological-unscented Kalman filter (hybrid SEIHCRDV-UKF) model for the prediction of COVID-19: Application on real-time data*, Chaos, Solitons and Fractals, *166* (2023).

[14] A. Sebbagh, C. Bencheriet, and S. Kechida, *A Stochastic Epidemiological SIRD-V Model With LSM-EKF Algorithm for Forecasting and Monitoring the Spread of COVID-19 Pandemic: Real Data*, IEEE Access, *12* (2024), 62047-62058.

[15] J. Song, H. Xie, G. Gao, Y. Zhong, C. Gu, and K. Choi, *Maximum likelihood-based extended Kalman filter for COVID-19 prediction*, Chaos, Solitons and Fractals, *146* (2021), 110922.

[16] T. Vasanthi, *Application of kalman filter model to hiv/aids epidemic*, American Psychological Association 7th edition, (2014).

[17] W. Wang, Y. Cai, Z. Ding, and Z. Gui, *A stochastic differential equation SIS epidemic model incorporating Ornstein–Uhlenbeck process*, Physica A: Statistical Mechanics and its Applications , *509* (2018), 921–936.

[18] Z. Yang, Z. Zeng, K. Wang, S. S. Wong, W. Liang, M. Zanin, and J. He, *Modified SEIR and AI prediction of the epidemics trend of COVID-19 in China under public health interventions*, Journal of Thoracic Disease, *12*(3) (2020), 165.
[19] G. Zhang, L. Zhiming, and D. Anwarud, *Stochastic SIQR epidemic model with Lévy jumps and three-time delays*, Applied Mathematics and Computation, *431* (2022).
[20] N. Zhiming, J. Daqing, C. Zhongwei, and M. Xiaojie, *Analysis of stochastic SIRC model with cross immunity based on Ornstein–Uhlenbeck process*, Qualitative Theory of Dynamical Systems, *22* (2023).
[21] X. Zhu, B. Gao, Y. Zhong, C. Gu, and K. S. Choi, *Extended Kalman filter based on stochastic epidemiological model for COVID-19 modelling*, Computers in Biology and Medicine, *137* (2021).